8063428

AACC

JACC/78

JOINT AUTOMATIC CONTROL CONFERENCE

October 18-20, 1978
Philadelphia, PA

Volume 2

Control Theory Meets the Real World of Applications

"CONTROL THEORY MEETS the REAL WORLD of APPLICATION"

~~TP13-2
AN
1978
V.2~~
TP13-53
A939
1978
V.2

8063428

Proceedings
of the

1978
Joint Automatic Control Conference
Volume II

Philadelphia, Pennsylvania
October 15 - 20, 197

图书馆
E8063428

SPONSORING SOCIETIES:
- AMERICAN INSTITUTE OF CHEMICAL ENGINEERS
- AMERICAN SOCIETY OF MECHANICAL ENGINEERS
- INSTITUTE OF ELECTRICAL AND ELECTRONICS ENGINEERS
- INSTRUMENT SOCIETY OF AMERICA
- SOCIETY OF MANUFACTURING ENGINEERS

PARTICIPATING SOCIETIES:
- AMERICAN INSTITUTE OF AERONAUTICS AND ASTRONAUTICS
- INSTITUTE OF TRAFFIC ENGINEERS
- SOCIETY FOR INDUSTRIAL AND APPLIED MATHEMATICS
- TECHNICAL ASSOCIATION OF THE PULP AND PAPER INDUSTRY

Published on behalf of the American Automatic Control Council by:
Instrument Society of America.

ISA

Library of Congress Number 65-67249
I.S.B.N. 87664-424-8 — Part II

All rights reserved:
Copyright © Instrument Society of America 1978
400 Stanwix Street
Pittsburgh, Pa. 15222

Printed in U.S.A.

MESSAGES FROM

GENERAL CHAIRMAN AND PROGRAM CHAIRMAN

On behalf of the JACC/78 Program Committee, we wish to express our sincere appreciation to the session developers and some two hundred authors who have contributed a great deal of their valuable time and energy to make this conference a meaningful and rewarding experience for the attendees.

We are extremely pleased with the wide range of the technical programs sponsored and contributed by all of the participating societies, particularly by the various committees of the American Automatic Control Council. We believe the program contains many outstanding papers both in theory and applications truly reflecting the major theme of this conference: "Control Theory Meets the Real World of Applications."

Finally, the 1978 JACC Program Committee wants to express its gratitude to the many individuals in the sponsoring and participating societies of American Automatic Control Council for their time and effort in putting together this 1978 program.

Harlan J. Perlis
General Chairman

Chun H. Cho
Program Chairman

CONTENTS PART 2

APPLICATION OF MATHEMATICAL MODELING TO DESIGN OF A PRACTICAL CONTROLLER FOR A COMMERCIAL SCALE FOSSIL POWER PLANT, Asok Ray and David A. Berkowitz. 1

SYSTEMS APPROACH FOR THE INCLUSION OF SOCIAL AND ENVIRONMENTAL CONSIDERATIONS ON THE ENERGY DECISION MAKING PROCESS, Robert B. Schainker* and G. Paul Grimsrud 13

DECENTRALIZED ELECTRIC TECHNOLOGIES: ENERGY AND ENVIRONMENTAL CONSIDERATIONS, Leif Isaksen, and Fred Ma 19

STABILITY AND CONTROL OF CHEMICALLY REACTING SYSTEMS – A REVIEW, Roger A. Schmitz 21

THE DYNAMICS AND CONTROL OF COAL GASIFICATION REACTORS, James Wei 39

AN APPLICATION OF SELF-TUNING REGULATORS TO CATALYTIC REACTOR CONTROL, T. J. Harris, J. F. MacGregor, and J. D. Wright. 41

DESIGN AND TUNING OF DEAD TIME COMPENSATORS, Z. J. Palmor and R. Shinnar 59

DYNAMICS OF THE MELT SPINNING PROCESS, Susumu Kase and Morton M. Denn 71

FLUIDIC APPLICATION OF PSEUDO-NOISE IN DYNAMIC CHARACTERIZATION OF INSTRUMENTS, Otis L. Updike and David B. McCallum 85

RATE LIMITING FILTER WITH LINEAR ZONE AND ITS APPLICATION TO DISTILLATION COLUMN CONTROL, Shinya Ochiai 99

COMPARISONS OF LINEAR SUB-OPTIMAL DEADTIME CONTROLS FOR A HEAT EXCHANGER PROCESS, L. H. Huang* and L. D. Durbin 109

ON-LINE SUBOPTIMAL FEEDBACK CONTROL OF A PACKED TRICKLE BED ABSORPTION COLUMN, Ali Cinar* and L. D. Durbin 123

QUADRATIC ERROR BASED PI CONTROL FEATURES WITH DEADTIME PROCESSES, L. H. Huang* and L. D. Durbin. 137

STATISTICAL PATTERN CLASSIFICATION USING CONTEXTUAL INFORMATION†, T. S. Yu and K. S. Fu 151

APPLICATIONS OF PATTERN RECOGNITION TO INDUSTRIAL INSPECTION*, T. Pavlidis. 159

MULTILEVEL SYNTAX ANALYSIS FOR GEOLOGICAL DATA COMPRESSION, H. E. Stephanou 165

此为试读，需要完整PDF请访问：www.ertongbook.com

NEW RESULTS IN IMAGE ALIGNMENT, T. R. Chow and T. C. Hsia 171

DIGITAL LINEAR PROCESSOR THEORY AND OPTIMUM MULTIDEMENSIONAL IMAGE RECONSTRUCTION, Sheldon S. L. Chang 177

CONTROL SENSORS FOR BIOMEDICAL SYSTEMS, Otis L. Updike. 195

HOMEOKINETIC PHYSICS – A THERMODYNAMIC BASIS FOR MODELLING COMPLEX SYSTEMS, A. S. Iberall 199

NEW CONTROL ALGORITHMS VIA BRAIN THEORY*, Baxter F. Womack and John P. Blanks 205

MULTIPARTITIONED SOLUTIONS FOR STATE AND PARAMETER ESTIMATION: CONTINUOUS SYSTEMS, D. G. Lainiotis and D. Andrisani II 215

NEW IDENTIFICATION ALGORITHMS AND THEIR RELATIONSHIPS TO MAXIMUM–LIKELIHOOD METHODS: THE PARTITIONED APPROACH, B. J. Eulrich, D. Andrisani II and D. G. Lainiotis 231

APPLICATION OF IDENTIFICATION ALGORITHMS TO AIRCRAFT FLIGHT DATA, K. S. Govindaraj, J. V. Lebacqz and B. J. Eulrich 247

ECONOMIC MODELING OF PROCESS MANAGEMENT AND CONTROL SYSTEMS, John W. Bernard, Malcolm C. Beaverstock and Lawrence B. Evans 259

CONTROL CONSIDERATIONS FOR AN IMAGE–TRACKING SYSTEM, E. S. McVey and D. E. Baker 277

MASTER CONTROL SYSTEM FOR THE CENTRAL RECEIVER SOLAR POWER PLANT*, D. M. Darsey, R. C. Rountree, R. R. Sheahan, M. A. Soderstrand and C. P. Winarski 287

OPTIMAL HALL CALL ASSIGNMENT METHOD OF ELEVATOR GROUP SUPERVISORY CONTROL SYSTEM, Kotaro Hirasawa, Sosiro Kuzunuki, Tatsuo Iwasaka and Takasi Kaneko 305

SIMULATION STUDY OF A ROLLING PLATFORM, C. R. Burrows 314

MANUFACTURING SYSTEMS ARCHITECTURE – AN AREA OF NEEDED DEVELOPMENT AND STANDARDIZATION REPORT OF THE ARC MANUFACTURING ARCHITECTURE OVERVIEW GROUP, Dr. M. E. Merchant 329

RESEARCH IN THE CAD/CAM SYSTEMS AND RELATED AREAS REPORT OF THE ARC CAD/CAM SYSTEMS GROUP, Edward E. Miller 341

NEEDS OF THE PERSONNEL AND HARDWARE INTERFACE FIELD REPORT OF COMPUTER AND PERSONNEL INTERFACT SYSTEMS GROUP, Thomas B. Sheridan 347

AUTOMATION NEEDS IN THE HEALTH SERVICES FIELD REPORT OF THE ARC HEALTH SERVICES GROUP, Herman R. Weed 355

SOLUTION OF SPARSE LINEAR EQUATIONS ARISING FROM POWER SYSTEM SIMULATION ON VECTOR AND PARALLEL PROCESSORS, Christopher Pottle 367

POWER SYSTEM DYNAMIC EQUIVALENTS, N. Narasimhamurthi and F. F. Wu 375

DECENTRALIZED CONTROL OF HARMONIC LEVELS IN POWER NETWORKS WITH DISPERSED CONVERTERS, Sarosh N. Talukdar and Ira J. Pitel 379

OPTIMAL DECOMPOSITION OF LARGE–SCALE NETWORKS, Jang G. Lee, William G. Vogt and Marlin H. Mickle. 389

FAULT TOLERANCE IN THE DESIGN OF DISTRIBUTED INTELLIGENCE DATA ACQUISITION CONTROL SYSTEMS, Charles W. Rose 401

©ISA 1978

APPLICATION OF MATHEMATICAL MODELING TO DESIGN OF A PRACTICAL CONTROLLER FOR A COMMERCIAL SCALE FOSSIL POWER PLANT

Asok Ray David A. Berkowitz

The MITRE Corporation
Bedford, Massachusetts

ABSTRACT

To design an improved fuel controller for an operating, 386 MW(e), oil-fired power generation system, a mathematical model of the plant was developed from fundamental principles to predict thermal-hydraulic transients. This controller was successfully implemented in the actual plant by replacing a portion of the original control system. The resulting minimum operating level of the system was thus reduced from 220 MW(e) to flash tank level of 130 MW(e), and the customary load rate of change during normal operation improved from approximately 2 MW/min to 9 MW/min.

INTRODUCTION

Due to rising fuel oil cost, economic dispatch favors operating large oil-fired power plants as load-followers and nuclear plants as baseload units. For example, in the Boston Edison Company system, two oil-fired 386 MW(e) once-through subcritical units were required to operate over a wider load range and to change output more rapidly following start-up of a new nuclear plant. However, with the original control scheme, the lower load limit was restricted to 220 MW(e) because of temperature and pressure instabilities. Figure 1 shows growing throttle pressure and temperature oscillations following a load reduction; output power had to be raised to regain stability, or the unit would be shut down. Furthermore, load rate-of-change was normally limited to 2 MW/min.

To identify the cause of the problems and to formulate an appropriate control algorithm, a dynamic model of the once-through subcritical steam generator and accessories was derived using established techniques [1,2]. The model was verified with plant data collected by a multichannel tape recorder and data acquisition system [3]. Simulation studies and test data suggested that low load instability was due to the fuel control system. Two specific design objectives for an improved fuel controller were defined: (1) the unit should operate stably at any load between 130 MW and 386 MW, with main steam temperature settling to set point value of 537.8°C (1000°F) less than 30 min after load change; and (2) main steam temperature excursions should be bounded within ± 5.6°C (± 10°F) for 9 MW/min load rate-of-change between 130 MW and 386 MW.

Application of linear control theory using the plant model led to successful design of a simple, practical fuel controller replacing a portion of the original control system. The resulting low load operating limit was reduced to flash tank level of 130 MW and the customary load rate-of-change during normal operation increased to 9 MW/min. Since May 1976, Unit No. 2 at New-Boston Station has operated with the revised control system. Because of improved performance, the plant is now automatically dispatched from the regional load control center.

SYSTEM DESCRIPTION

Plant ratings for New-Boston Unit No. 2 are given in Table 1. It incorporates a once-through subcritical Babcock & Wilcox steam generator. Heat exchanger dimensions are given in Table 2. The furnace has 24 guns for oil firing and two forced draft fans. Two gas recirculating fans, drawing flue gas just ahead of the air preheaters, discharge to recirculating ducts below the burners and to tempering ducts near the top of the furnace radiation section; the ratio of flue gas distribution between recirculating and tempering ducts can be adjusted manually or automatically.

The balance of plant is essentially of conventional reheat type except that the main feedwater pump is driven from the turbine generator shaft through a fluid drive mechanism. Feedwater pump speed is modulated by the fluid drive to control feedwater flow or pressure.

Normal plant design operating range is from 100 percent to 33 percent rated feedwater flow rate. Below 33 percent, a portion of main steam is diverted through the flash tank.

MATHEMATICAL MODEL

A mathematical description or model of the process provides an understanding of its dynamics and forms the basis for plant controller design and evaluation. The model must satisfy two criteria:

1. Optimum model complexity, i.e., the model should be no larger nor more complex than is necessary for the purposes at hand;

2. Numerical solutions of the model equations must be readily obtained.

The once-through subcritical steam generator, which is the most significant plant component, was modelled using a first principles approach based on thermodynamic phase information (i.e. compressed water, two-phase mixture, and superheated steam corresponding to economizer, evaporator, and superheater, respectively). This concept was first introduced by Adams et al.[1] who modelled a coal-fired once-through subcritical steam generator, then linearized the model for analog simulation. Ray and Bowman extended this technique for digital simulation of such a steam generator in a gas-cooled nuclear power plant [2]. A nonlinear dynamic model of the New-Boston Unit No. 2 steam generator was derived from the same concept, but with some modifications. The primary modeling objective was to represent main steam temperature dynamics for the purpose of analytical design of a fuel controller.

The phase boundaries (i.e., locations of saturated water and steam) vary with time. Although rate-of-change of these boundary locations may be high under transient conditions, the range of variation is relatively narrow. Thus, the nonlinear model was structured with fixed thermodynamic phase boundaries. Further, since steam temperature is strongly influenced by heat transfer rate, the superheater region was modelled in primary and secondary superheater sections. When the nonlinear model was linearized at different operating points, model parameters for the linearized models were adjusted corresponding to the length of the phase regions - the economizer, evaporator and superheater. Model results were made to agree with steady-state plant data at several operating levels.

The nonlinear, time-invariant, continuous-time model has the form

$$\dot{\underset{\sim}{x}} = \underset{\sim}{f}(\underset{\sim}{x};\underset{\sim}{u}) \quad (1)$$

$$\underset{\sim}{y} = \underset{\sim}{g}(\underset{\sim}{x};\underset{\sim}{u}) \quad (2)$$

$\underset{\sim}{x}$ is the state vector, with the elements:

x_1 = secondary superheater average metal temperature
x_2 = secondary superheater average steam enthalpy
x_3 = secondary superheater average steam density
x_4 = primary superheater average metal temperature
x_5 = primary superheater average steam/water enthalpy
x_6 = primary superheater average steam/water density
x_7 = evaporator (two-phase section) average metal temperature
x_8 = economizer (subcooled water section) average metal temperature
x_9 = economizer (subcooled water section) average water enthalpy

$\underset{\sim}{u}$ is the input (control) vector, whose elements are:

u_1 = fuel flow
u_2 = feedwater flow
u_3 = feedwater enthalpy (at the inlet of economizer)
u_4 = throttle pressure

$\underset{\sim}{y}$ is the output vector. To design a fuel controller for maintaining constant main steam temperature, only two elements were chosen as output variables:

y_1 = main steam temperature
y_2 = main steam flow

Model equations (1) and (2) were linearized at seven steady-state operating points in the 45-100 percent load range. System eigenvalues (i.e. eigenvalues of the A-matrix) were evaluated for the seven linearized models; their root locus plot is shown in Figure 2. Two dominant eigenvalues (closest to the imaginary axis) monotonically decrease in magnitude with load reduction. By examination of the linearized models, main steam temperature was found to be closely associated with these two eigenvalues which are strongly influenced by energy storage in the primary and secondary superheater tube walls.

The original control system was modelled and incorporated in the plant model. The linearized closed loop system yielded a pair of system eigenvalues very close to the imaginary axis. With decreasing load, these eigenvalues monotonically drifted to the right-half plane. Closed loop system stability improved with certain changes in fuel controller parameters, but at the cost of response time. It was felt that a revised fuel control scheme was required to satisfy the design objective.

CONTROLLER DESIGN CONCEPTS

In the boiler following mode, electrical power output changes are effected by manipulating governor valves, whose displacement directly influences main steam flow and pressure which, in turn, cause feedwater flow to change. Thermal-hydraulic processes in the steam generator are dependent on both feedwater and fuel flow. Following a load change, fuel flow must be compensated for feedwater flow variations to avoid undesirable deviations in main steam temperature. Thus, feedwater flow W_{fw} is treated as an independent variable. Fuel flow is also dependent on other variables (such as feedwater temperature, draft air flow, etc.). The control design task is to structure the dependence of fuel flow on several independent variables (feedwater flow being the most significant) such that main steam temperature does not deviate beyond specified limits for permissible variations of the independent variables. This analytical relationship is known as the feedforward function [4], which acts as a fast, coarse controller. In addition, a relatively slow feedback loop is provided to compensate for modeling errors and spurious noise (i.e., to hold main steam temperature at the set point under steady-state conditions).

Feedforward Function

The feedforward function has been constructed in two parts: static and dynamic. The static part calculates steady-state fuel flow required for thermal equilibrium in the steam generator. To find the steady-state fuel flow, u_1, for achieving a desired value of main steam temperature T_d, set $\dot{\underset{\sim}{x}} = \underset{\sim}{0}$ and $y_1 = T_d$ in equations (1) and (2), respectively, which results in eleven equations.

$$\begin{aligned}
0 &= f_1(x_1, \ldots, x_9; u_1, \ldots, u_4) \\
&\cdot \quad \cdot \\
&\cdot \quad \cdot \\
&\cdot \quad \cdot \\
0 &= f_9(x_1, \ldots, x_9; u_1, \ldots, u_4) \qquad (3) \\
T_d &= g_1(x_1, \ldots, x_9; u_1, \ldots, u_4) \\
y_2 &= g_2(x_1, \ldots, x_9; u_1, \ldots, u_4)
\end{aligned}$$

With u_2, u_3, u_4 given, equations (3) could be solved for the eleven unknowns u_1, y_2, x_1, x_2, x_3, x_4, x_5, x_6, x_7, x_8, and x_9. In practice, however, equations (3) are very difficult to solve in closed form because f and g are nonlinear functions that involve implicit loops. Analog solution would also be too complex to be practical. To circumvent this problem, steady-state fuel flow demand was obtained by a simple energy balance in the furnace and steam generator as shown in Figure 3. Heat delivered by feedwater, reheat attemperating water, high pressure turbine exhaust steam, draft air and fuel matches heat removed by flue gas, steam and fixed loss to the environment, under thermal equilibrium. If, at steady-state, reheater load is assumed proportional to feedwater flow, and main steam enthalpy has the desired constant value, then fuel flow W_{fo} can be expressed in terms of feedwater flow W_{fw} and temperature T_{fw} in the following form [5]:

$$W_{fo} = K[(a + bT_{fw})W_{fw} + c] \qquad (4)$$

a, b and c are constants whose physical meaning is discussed in reference 5.

For the dynamic portion of the feedforward function, main steam temperature transfer functions with respect to feedwater flow, W_{fw}, and fuel flow, W_{fo}, can be obtained from a linearized version of equations (1) and (2) as,

$$\frac{T_{ms}}{W_{fw}}(s) = G_1(s) = K_1 \frac{\prod_{i=1}^{m_1}(1 + s/z_{1i})}{\prod_{j=1}^{n_1}(1 + s/p_{1j})}, \quad m_1 \le n_1 \tag{5}$$

and

$$\frac{T_{ms}}{W_{fo}}(s) = G_2(s) = K_2 \frac{\prod_{i=2}^{m_2}(1 + s/z_{2i})}{\prod_{j=2}^{n_2}(1 + s/p_{2j})}, \quad m_2 \le n_2 \tag{6}$$

The transfer function of W_{fo} with respect to W_{fw}, subject to the constraint that, T_{ms} is constant, is

$$\frac{W_{fo}}{W_{fw}}(s) = -\frac{G_1(s)}{G_2(s)} = -\frac{K_1}{K_2} \frac{\prod_{i=1}^{m_1}(1 + s/z_{1i}) \prod_{j=1}^{n_2}(1 + s/p_{2j})}{\prod_{i=1}^{m_2}(1 + s/z_{2i}) \prod_{j=1}^{n_1}(1 + s/p_{1j})} \tag{7}$$

Since the model is ninth order, the number of any transfer function poles cannot exceed 9. Therefore, $\max(m_1, m_2, n_1, n_2) \le 9$.

The coefficient of W_{fw} in the linearized form of Equation (4) is equal to the steady-state gain $(-K_1/K_2)$ of equation (7) if equations (1) and (2) are linearized at the same point as equation (4). We define dynamically compensated feedwater flow, W_{dc} as

$$W_{dc}(s) = \frac{\prod_{i=1}^{m_1}(1 + s/z_{1i}) \prod_{j=1}^{n_2}(1 + s/p_{2j})}{\prod_{i=1}^{m_2}(1 + s/z_{2i}) \prod_{j=1}^{n_1}(1 + s/p_{1j})} W_{fw}(s) \tag{8}$$

Parameters z and p are functions of the load conditions at which equations (1) and (2) are linearized. Replacing W_{fw} by W_{dc} in equation (4) includes fuel flow dynamics with respect to feedwater flow in the feedforward function.

As discussed earlier, main steam temperature is strongly influenced by two dominant eigenvalues (see Figure 2). Therefore, the transfer function order in equations (5) and (6) can be approximated by 2 or less. Further, test data and model results, as well as physical reasoning, show no immediate change in T_{ms} following a step change in either W_{fo} or W_{fw},, which means that m_1 and m_2 must be less than n_1 and n_2, respectively. Thus, $\max(n_1, n_2) \le 2$ and $\max(m_1, m_2) \le 1$ in equation (8), and an analog simulation of the transfer function can be constructed by at most three cascaded lag units.

The distributed thermal-hydraulic process in the superheater has been represented by two lumped sections, and the two dominant eigenvalues are closely associated with these two sections. As a first step in the feedforward dynamic compensator design, the two dominant eigenvalues are approximated by a single eigenvalue resulting in the simplified transfer function structures,

$$G_1(s) = \frac{K_1}{1 + \tau_{fw}s} \quad \text{and} \quad G_2(s) = \frac{K_2}{1 + \tau_{fo}s}$$

which reduce equation (8) to

$$\frac{W_{dc}}{W_{fw}}(s) = \frac{1 + \tau_{fo}s}{1 + {}_{fw}s} \tag{9}$$

τ_{fo} and τ_{fw} are functions of plant load. The transfer function in equation (9) can be constructed by a single lag unit, simplifying equipment installation.

此为试读,需要完整PDF请访问: www.ertongbook.com

Values of τ_{fo} and τ_{fw} were identified at several load levels using the linearized model frequency responses. They were confirmed by values determined from the nonlinear model in the time domain using a small signal perturbation technique. Thus, results obtained by frequency-domain and time-domain identification were in fairly close agreement.

The feedforward function with analytically determined values of τ_{fo} and τ_{fw} was verified experimentally at different load levels. Results indicated that the dynamic compensator structure in equation (9) was adequate for stabilizing initial oscillations that occur shortly after the disturbance is applied. Slower transients and steady-state drift are overcome by feedback control (discussed in the next section).

Although τ_{fo} and τ_{fw} can be expressed as functions of load, they are not readily convertible to analog circuit representation. If the functional dependence of τ_{fo} and τ_{fw} on plant load could be avoided, equipment implementation would be simpler, resulting in improved reliability. Fixed average values of 200 and 150 seconds, respectively, for τ_{fo} and τ_{fw} were tested over the full operating range, and initial oscillations were within permissible limits. The transfer function for the feedwater flow dynamic compensator (which was implemented in the plant) is, therefore,

$$\frac{W_{dc}}{W_{fw}}(s) = \frac{1 + 200s}{1 + 150s} \tag{10}$$

Feedwater temperature T_{fw} is also compensated dynamically. The transfer function between main steam and feedwater temperatures is primarily the result of a transport delay, τ_x, in the steam generator tubes. Following a derivation similar to the feedwater flow dynamic compensator, the transfer function for W_{fo} with respect to T_{fw} is approximately

$$\frac{W_{fo}}{T_{fw}}(s) = \frac{K_3(1 + \tau_{fo}s)}{\exp(\tau_x s)} \tag{11}$$

For equipment simplification, equation (11) was further approximated by

$$\frac{W_{fo}}{T_{fw}}(s) = \frac{K_3}{1 + \tau s} \tag{12}$$

With $\tau = 120$ sec, tests were conducted at different load levels in which a disturbance in T_{fw} was applied by bypassing the high pressure feedwater heaters. The results were satisfactory. The transfer function for the feedwater temperature dynamic compensator (which was implemented in the plant), is therefore

$$\frac{T_{dc}}{T_{fw}}(s) = \frac{1}{1 + 120s} \tag{13}$$

Using equations (10) and (13) in the time domain form, the feedforward function of equation (4) is modified to include dynamic compensation.

$$W_{fo} = K[(a + bT_{dc})W_{dc} + c] \tag{14}$$

Feedback Controller

A conventional proportional-integral-derivative (P-I-D) controller was used for feedback control of main steam temperature. The error signal input to the proportional-integral (P-I) controller is the difference between set point and measured value of main steam temperature. A weighted derivative of main steam temperature is added to the P-I controller output to obtain the P-I-D function. The signal required to drive the fuel flow actuator is generated by multiplying the P-I-D controller output with the dynamically compensated feedforward signal from equation (14). A multiplier is incorporated to reduce effective feedback gain as plant load decreases. As shown in Figure 2, the dominant time-constants (i.e., inverse of the dominant eigenvalues) increase as plant load decreases, indicating that feedback can be made stronger at high load than at low load. Controller parameters must be adjusted with load change to ensure fast and stable operation. In this case, effective controller gain associated with fuel flow actuator drive, which is the product of true controller gain and feedforward signal, monotonically decreases with load.

To design the feedback controller, a Bode plot of main steam temperature versus fuel flow was generated from the plant model at full load and is shown in Figure 4. With performance criteria of gain margin = 0.5 and phase margin = 45°, the P-I-D controller parameters were evaluated using standard frequency-domain design techniques for linear time-invariant single-input single-output systems [6]. The analytically evaluated parameters were used initially to operate the plant and were subsequently readjusted as operating experience increased. The Laplace transform for the P-I-D controller impulse response is

$$0.4(1 + \frac{1}{\tau_i s} + \tau_d s) \tag{15}$$

where τ_i = 500 sec and τ_d = 176 sec.

CONTROLLER IMPLEMENTATION

The revised fuel controller was integrated with the original control system using spare modules installed on an adjacent empty panel. It consists of two lag units, two servomultipliers, two potentiometers, four sum units, one integrator and one derivative unit as shown in Figure 5.

Lag unit L1 is the dynamic compensator for feedwater temperature (see equation (13)); lag unit L2 and sum unit A2 are for feedwater flow (see equation (10)). Sum unit A1 output represents the fuel flow signal generated by the feedforward function (see equation (14)). Input 1 at A1 is proportional to the product of feedwater flow and temperature; input 2 is proportional to feedwater flow, only. Inputs 3 and 4 represent the fixed term of equation (14), which includes air flow heat load. Sum unit A3 output is proportional to the term ($W_{air} - \xi W_{fo}$) where ξ is the air-fuel ratio. For plant load above 200 MW, air flow is proportional to fuel flow, and the output of A3 is practically zero; for lower loads, air flow is held constant corresponding to 200 MW although fuel flow diminishes. The output of sum unit A4 is the feedback control signal which is multiplied with the A1 output to yield the fuel flow actuator drive signal. Main steam temperature error ΔT_{ms} is summed with its own integral from I1 and the derivative of T_{ms} from D1. The nominal servomultiplier position at A1 output can be adjusted by varying input 4 to A4.

RESULTS AND DISCUSSION

The fuel controller, described above, was installed at New-Boston Unit No. 2. Test results show stable operation in the load range of approximately 130 MW to 386 MW, and load rate-of-change exceeding 9 MW/min with main steam temperature variations within permissible limits (±5.6°C). Figure 6 shows a typical load pick up at more than 9 MW/min. Main steam temperature, which had been 543.3°C (1010°F), subsequently rose to 548.9°C (1020°F), and then returned to 543.3°C (1010°F), while power increased from approximately 180 MW to 330 MW. Later on, main steam temperature set point was adjusted bringing the main steam temperature down to 537.8°C (1000°F). In this case, load change was accomplished manually by the operator. In other tests, load rate-of-change up to 12 MW/min on automatic dispatch has been accomplished with permissible temperature fluctuation for both load increase and decrease.

A high pressure feedwater heater leak occurred shortly after the new fuel controller was installed. The leaky heater was bypassed and main steam temperature set point reduced to 510°C (950°F). Under this operating condition, a 10 MW/min load rate-of-change was achieved and low load stability was retained with no adjustment of control parameters. Prior to installation of this controller, main steam temperature exhibited sustained oscillations with peak amplitude of ± 2.8°C (± 5°F) and a period of about 10 min.

During another test, a high pressure heater failure caused a 33.3°C (60°F) feedwater temperature change in 5 min while the unit was operating at a fixed load. Previously, this type of disturbance could trip the unit. With the new controller, operation continued and main steam temperature excursions were held within ± 8.3°C (± 15°F).

Boston Edison Company operating personnel have gained confidence in load maneuvering with the new fuel controller. Load dispatch has been automated and New-Boston Unit No. 2 is now remotely controlled by the regional load control center.

CONCLUSIONS

A mathematical model for an oil-fired 386 MW(e) once-through subcritical steam power plant was formulated using established techniques. The model was used to design a relatively simple fuel controller which was installed in the plant replacing a part of the original control system. Significant improvement in stability and load rate-of-change was achieved, and it was possible to put the plant on automatic dispatch.

This study shows that first-principles modeling and linear control theory can be applied for designing simple and practical controllers to improve system performance. The overall method of analysis presented here, although specifically related to a once-through subcritical steam generator, is also applicable to other processes.

ACKNOWLEDGEMENT

The authors acknowledge the participation of Dr. Y. Lin and Mr. R. S. Nielsen in this project, and are grateful to New Boston Station personnel for their cooperation in conducting tests at the station.

REFERENCES

1. Adams, J., Clark, D. R., Louis, J. R. and Spanbauer, J. P., "Mathematical Modeling of Once-through Boiler Dynamics", IEEE Trans., PAS, Vol. PAS-84, No. 2, Feb. 1965, pp. 146-156.

2. Ray, A. and Bowman, H. F., "A Nonlinear Dynamic Model of a Once-through Subcritical Steam Generator", Journal of Dynamic Systems, Measurements, and Control, Trans. ASME, Ser. G., Vol. 98, No. 3, Sept. 1976, pp. 332-339.

3. Berkowitz, D. A. and Nielsen, R. S., "Techniques for Improving Existing Plants", Presented at 96th Winter Annual Meeting (Automatic Control, Section 6 - Panel on Dynamics and Control of Large Thermal Power Stations), Nov. 30 - Dec. 5, 1975, Houston, Tex.

4. Shinsky, F. G., Process Control Systems, McGraw Hill, New York, 1967

5. Lin, Y., Nielsen, R. S. and Ray, A., "Fuel Controller Design in a Once-through Subcritical Steam Generator System", Journal of Engineering for Power, Trans. ASME, Vol. 100, No. 1, Jan. 1978, pp. 189-196.

6. Kuo, B. C., Automatic Control Systems, Prentice-Hall, Englewood Cliffs, 1967.

Table 1. Plant Ratings

Electrical Power	386 MW	
Throttle steam pressure	1.655×10^7 N/m^2 g	(2400 psig)
Throttle steam temperature	537.8°C	(1000°F)
Reheat steam temperature	537.8°C	(1000°F)

Table 2. Boiler Heat Exchanger Dimensions

Exchanger	Surface Area	Water Holding Capacity
Furnace	1,717 m^2	51,040 kg
Primary Superheater	11,890	111,100
Secondary Superheater	1,505	18,720
Reheat Superheater	3,756	60,050
Economizer	5,481	57,960

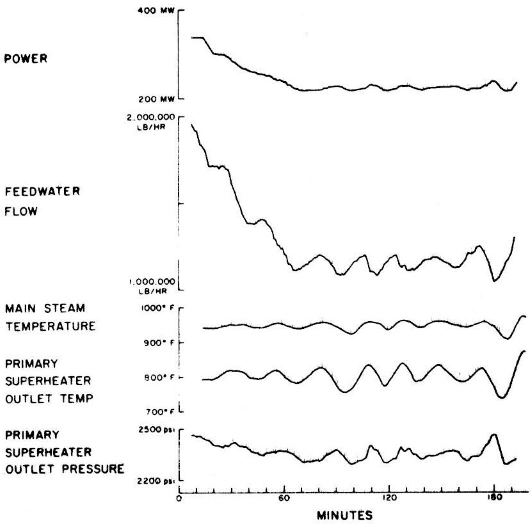

Figure 1 TEMPERATURE AND PRESSURE INSTABILITY AT LOW LOAD

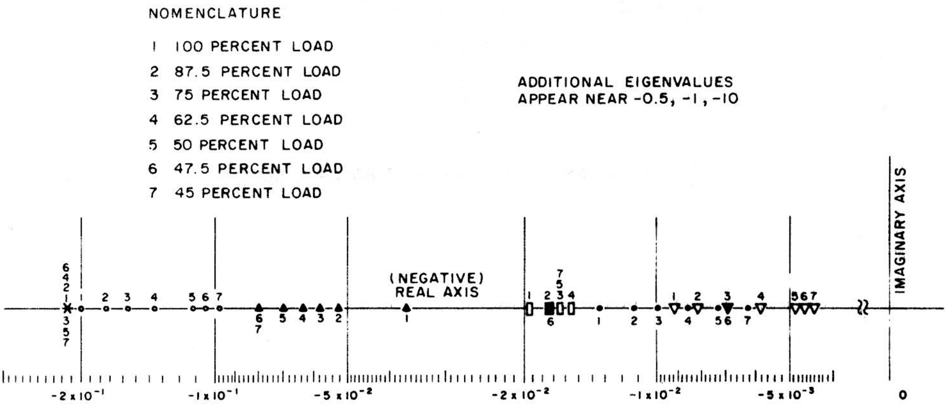

Figure 2 ROOT LOCUS PLOT SHOWING VARIATION IN SYSTEM EIGENVALUES OF BOILER MODEL WITH LOAD

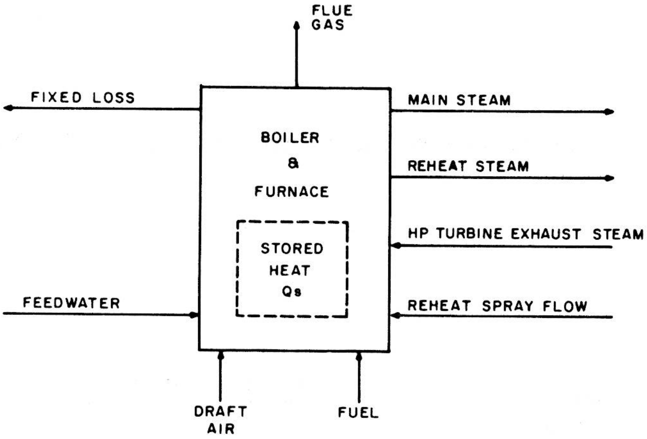
FLUE GAS
FIXED LOSS
MAIN STEAM
BOILER
&
FURNACE
REHEAT STEAM
HP TURBINE EXHAUST STEAM
STORED
HEAT
Qs
FEEDWATER
REHEAT SPRAY FLOW
DRAFT AIR
FUEL

Figure 3 FURNACE-BOILER HEAT BALANCE SCHEME

此为试读,需要完整PDF请访问: www.ertongbook.com